Advances in Natural Sciences:
Nanoscience and Nanotechnology

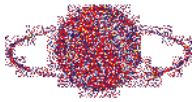

**PAPER**

# $LaCrO_3$ nano photocatalyst: the effect of calcination temperature on its cellulose conversion activity under UV-ray irradiation

IOP Publishing | Vietnam Academy of Science and Technology Advances in Natural Sciences: Nanoscience and Nanotechnology

Adv. Nat. Sci.: Nanosci. Nanotechnol. **10** (2019) 015009 (8pp) https://doi.org/10.1088/2043-6254/ab0280

# $LaCrO_3$ nano photocatalyst: the effect of calcination temperature on its cellulose conversion activity under UV-ray irradiation

**Rudy Situmeang[1], Matthew Tamba[1], Erwin Simarmata[1], Tria Yuliarni[1], Wasinton Simanjuntak[1], Zipora Sembiring[1] and Simon Sembiring[2]**

[1] Department of Chemistry, University of Lampung, Bandar Lampung, Indonesia
[2] Department of Physics, University of Lampung, Bandar Lampung, Indonesia

E-mail: rudy.tahan@fmipa.unila.ac.id

Received 31 October 2018
Accepted for publication 22 January 2019
Published 26 February 2019

**Abstract**

Nano-photocatalysis offers an environmentally friendly method, low cost process, and easy handling operation. In addition, converting cellulose as an abundant waste of agricultural side-product into glucose and alcohol sugar is interesting and challenging. $LaCrO_3$ nano photocatalyst was prepared using sol-gel and freeze-drying method. After the gelation and freeze-drying process, the precursors were subjected directly to the calcination treatment at 600, 700, and 800 °C, respectively. Then, the samples were subsequently characterized using x-ray diffraction (XRD), diffuse reflectance UV–vis spectroscopy (DRS), Fourrier transform infrared spectroscopy (FTIR), scanning electron microscopy (SEM) and transmission electron microscope (TEM). The results proved that $LaCrO_3$ crystalline phase is formed and its grain size is approximately 30 nm. DRS analysis also proved that band gap energy is affected by temperature calcination, and its value is around 2.9 eV. Its activity test said that the calcination temperature affected the conversion of cellulose. The cellulose conversion is more than 20% with the yield of alcohol sugar more than 600 ppm in 45 min exposure of the UV irradiation.

Keywords: nano, cellulose, sol-gel, alcohol sugar, perovskite

## 1. Introduction

A photocatalyst is a catalyst that can function while it is subjected to the radiation rays so that electrons are promoted from the HOMO to the LUMO level due to a reaction happened. Compound that can be used as a photocatalyst is a material that has a band-gap energy in the range of the radiation light applied [1–3]. In general, materials that can be used as photocatalysts have semiconductor properties [4–6]. One of them is perovskite materials.

Perovskite compounds are widely used in the field of catalysts [7–9], sensors [10–12], optics [13, 14], and electronics [15, 16]. The widespread use of the material is due to its unique properties, such as electric conductivity [17, 18], high-temperature resistors [19, 20], refractive indexes [21, 22], and semiconducting properties [23, 24]. In the field of catalysis, particularly photocatalysis, perovskite compounds are also used to decompose dye pollutants in water [25, 26]. In cellulose conversion, $TiO_2$ photocatalyst has been used to decompose cellulose into mixtures of hydrogen, carbon dioxides, glucose, and formic acid under UV irradiation by 93.4% of C-balance [27]. On the other hand, $LaTiO_2N$ perovskite was used to oxidize water into oxygen with the yield of 99% [28], whereas $LaFe_{0.8}Cu_{0.2}O_3$ composite films abled to decompose methyl orange dye under the visible light by 67% [29]. Given the unique characteristics and excellent ability to decompose dye pollutants, the perovskite material is certainly an opportunity to be applied on the breakdown of cellulose into alcohol sugar compounds.

Cellulose is a material that is very abundant in nature and can be used as a source of raw materials for energy and the production of more useful chemical compounds. In Indonesia, waste of the cellulose is very abundant which come from agricultural industrial waste such as cassava, sugar cane, pineapple, palm, and banana. One of the cellulose sources whose utilization has not optimal yet is banana peel which

 

reaches $6 \times 10^5$ tons yearly [30, 31] and the utilization of cellulose waste in Indonesia have begun to emerge [32–36]. So in this study the conversion of nano-cellulose into alcohol sugar with the $LaCrO_3$ catalyst under UV irradiation was reported. The preparation and characterization of $LaCrO_3$ have been reported on the previous articles [37, 38].

## 2. Materials and methods

### *2.1. Materials*

Materials used in this work were pectin powder, banana peel (waste from a domestic market), hydrated lanthanum nitrate ($La(NO_3)_3.6H_2O$), and hydrated chromium nitrate ($Cr(NO_3)_3.9H_2O$), and ammonia. All salt material is a commercial product of Merck.

### *2.2. Methods*

*2.2.1. Preparation of nano-cellulose material.* The banana peel was washed and then heated in an oven at 60 °C until the weight of banana peel was constant. Furthermore, the dry banana peel was mashed using a blender and sieved with a size of 125 meshes. Then, banana peel powder taken as much as 50 g, put into a round flask. Into the flask was added a solution of NaOH 4% until all parts of the powder were in solution. Then, the solution was carried out reflux at a temperature of 100 °C–120 °C for 2 h. The results of the reflux were filtered and washed with distilled water to remove lignin and hemicellulose. The washing fiber was then dried before the bleaching process. The bleaching process was carried out by mixing of 50 grams of cellulose fiber, 400 ml of 1.7% $NaClO_2$ solution, acetic acid and distilled water then refluxed at a temperature of 110 °C–130 °C for 4 h. After refluxing, the mixture was cooled to room temperature and then centrifuged and washed simultaneously until a white cellulose solid was obtained.

*2.2.2. Preparation of nano $LaCrO_3$.* Solid $LaCrO_3$ was prepared by dissolving specified mass of $La(NO_3)_3.9H_2O$, and $Cr(NO_3)_3.6H_2O$, respectively in 100 ml pectin solution 4%. The mixture was stirred until homogeneous solution was obtained, and then freeze-dried. Dry samples were calcined to 600, 700, and 800 °C using the temperature program with temperature increase of 2 °C $min^{-1}$. While the final temperature has been reached, the calcination temperature is attained for 2 h.

*2.2.3. Characterization of $LaCrO_3$ nanomaterial.* The material characterization determined by x-ray diffractometer (XRD) for structural and crystalline phase identification, scanning electron microscope (SEM) for analyzing surface morphology, transmission electron microscopy (TEM) for structural dan grain size identification, and UV–diffuse reflectance spectroscopy UV–vis for measuring bandgap energy and Fourrier transform infrared spectroscopy (FTIR) for functional groups identification.

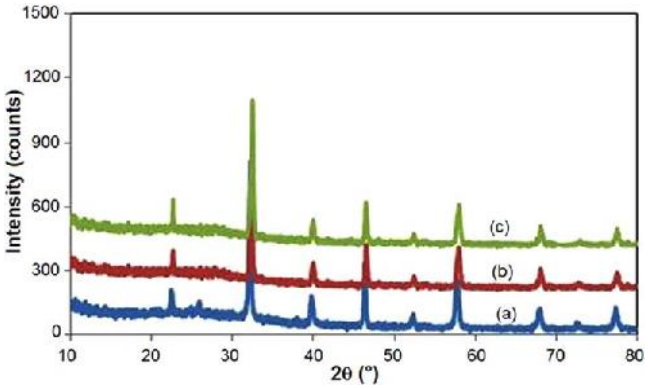


**Figure 1.** Diffractogram of $LaCrO_3$ calcined at (a) 600 °C, (b) 700 °C, and (c) 800 °C.

## 3. Results and discussion

### *3.1. X-ray diffraction analysis of $LaCrO_3$*

Based on the diffractogram as shown in figure 1, it is clear that the crystalline phase formed is perovskite $LaCrO_3$ although the structure is different. The $LaCrO_3$ calcined at 600 °C gave a cube shape of $LaCrO_3$, while $LaCrO_3$ calcined at 700 and 800 °C were orthorhombic with cell parameters slightly different, as explained by Situmeang *et al* in his previous article [37, 38].

### *3.2. Diffuse reflectance spectroscopy UV–vis analysis of $LaCrO_3$*

Figure 2 shows that the $LaCrO_3$ calcined at 600, 700 and 800 °C gave a positive response to both visible and UV light treatments. Figure 2(a) shows the UV absorption occurs in the region 200–400 nm with a maximum absorption at a wavelength greater than 350 nm. Then, the absorption of visible light at a wavelength of about 650 nm is seen although relatively small. Light absorption shown by the $LaCrO_3$ indicates that the material can work in visible and UV light areas. Furthermore figure 2(b) states that reflection of UV light occurs starting at wavelengths above 350 nm and continues to increase, especially for the $LaCrO_3$ prepared at 800 °C. Whereas, the $LaCrO_3$ prepared both 600 and 700 °C, show the optimum reflection at a wavelength of about 500 nm. It is clear that the higher the calcination temperature for the formation of $LaCrO_3$ the greater the band gap energy.

### *3.3. TEM and SEm analysis of $LaCrO_3$*

The crystallite appearance of $LaCrO_3$ calcined at 600, 700, and 800 °C in figure 3 showed that the granules formed were generally agglomerated. It could be still seen in the certain location, especially in figures 3(a) and (c), the small granules with nano size existed. The size of the $LaCrO_3$ grains can be determined by comparing the shape of the crystalline phase

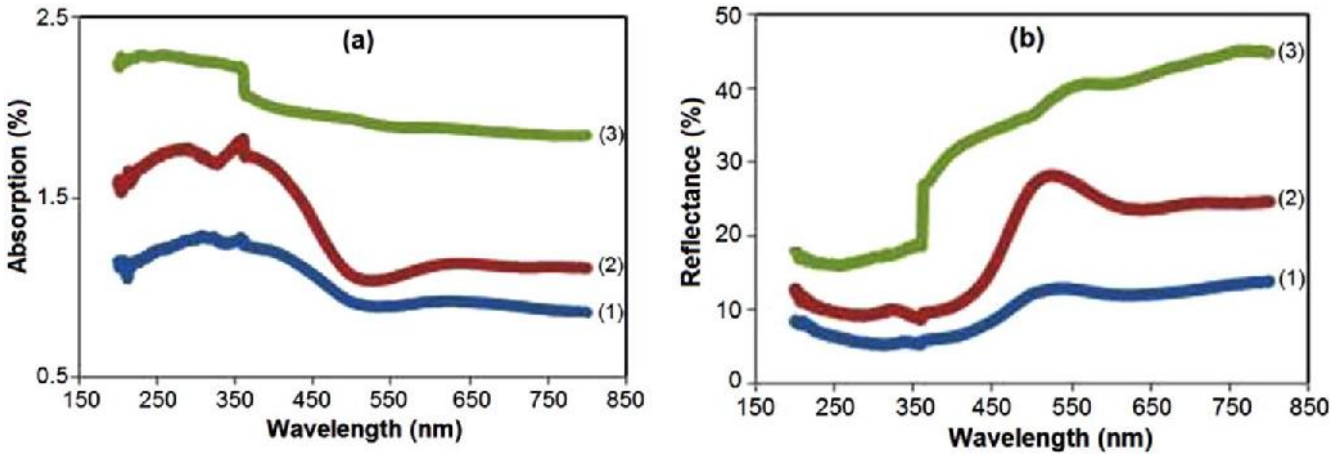


**Figure 2.** Absorption (a) and reflectance (b) features of $LaCrO_3$ calcined at (1) 600 °C, (2) 700 °C, and (3) 800 °C.

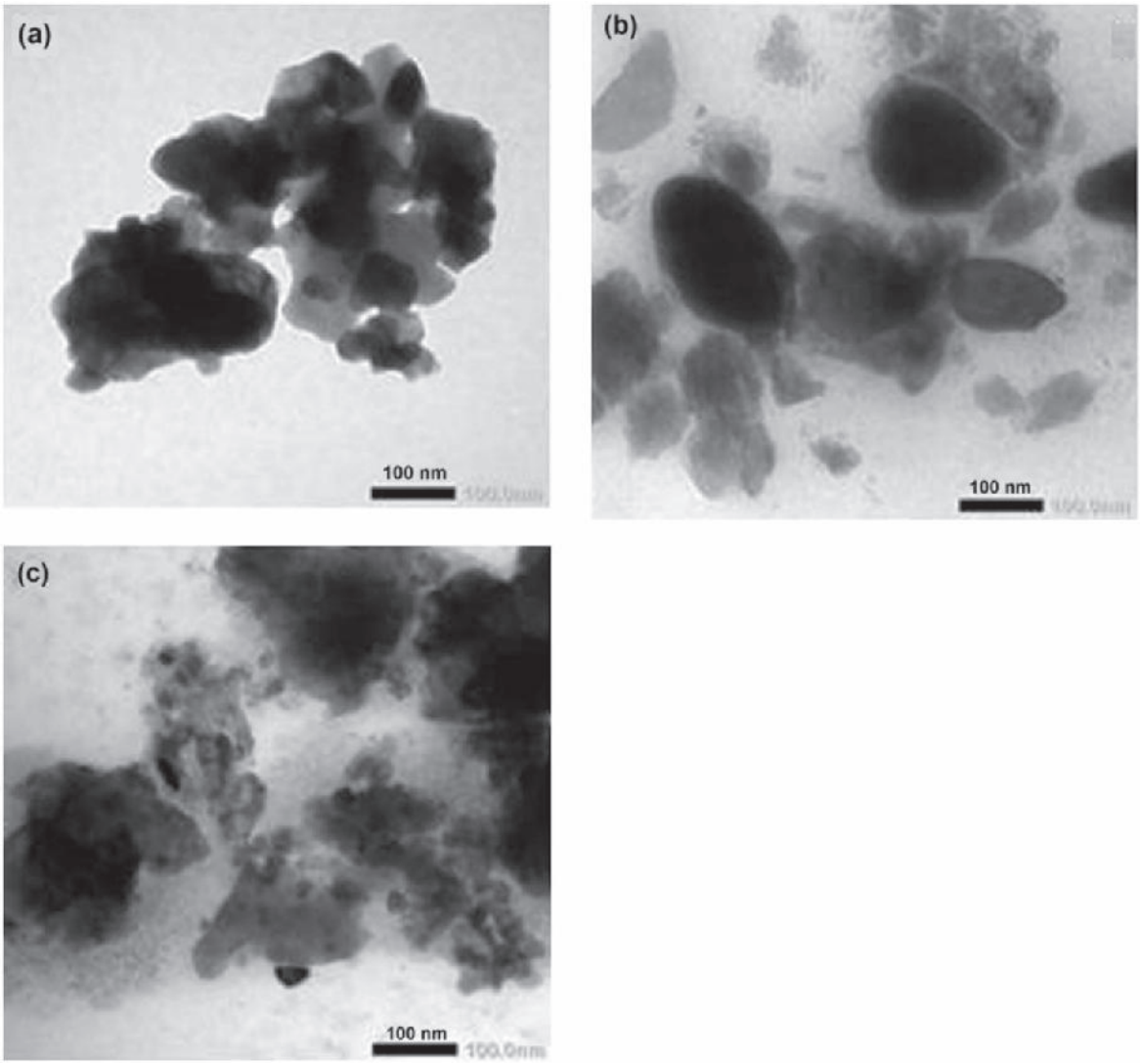


**Figure 3.** TEM micrographs of $LaCrO_3$ calcined at (a) 600 °C, (b) 700 °C, and (c) 800 °C.

and the size of the scale of 100 nm in figure 3. Therefore, the size of $LaCrO_3$ is around 50 nm.

The surface morphology of $LaCrO_3$ material calcined at temperatures of 600, 700 and 800 °C was analyzed using SEM as shown in figure 4. In figure 4(a) $LaCrO_3$ is formed homogeneously and forms a hollow network. The shape of the cube appears to dominate the surface area but the spherical shape and cube extends on one side, although it is minor.

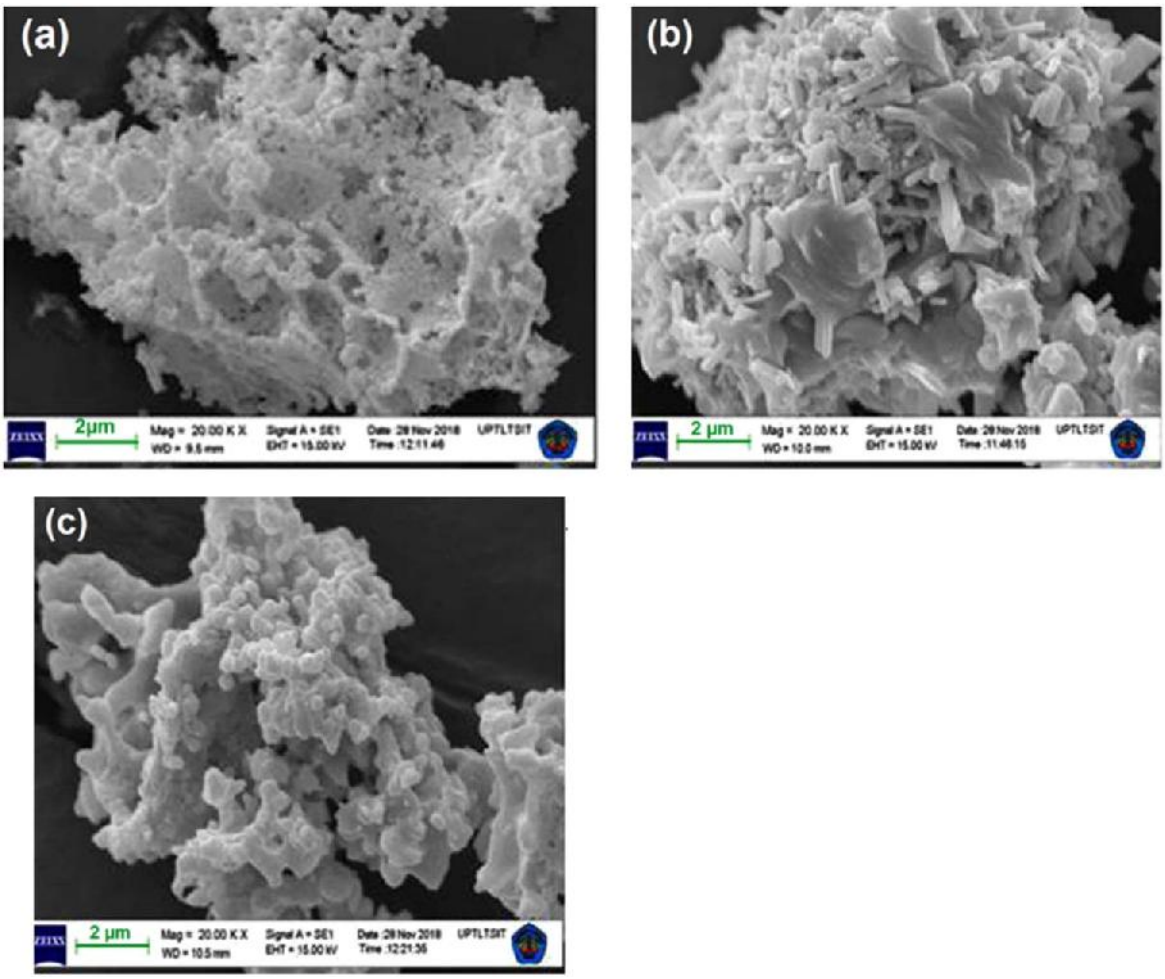


**Figure 4.** SEM images of $LaCrO_3$ calcined at (a) 600 °C, (b) 700 °C, and (c) 800 °C.

Furthermore, in figure 4(b) there are various crystalline such as hexagonal, orthorhombic, irregular and spherical phases. In general, it can be said that the form of orthorhombic is dominant. Meanwhile, in figure 4(c) it appears that the rhombhohedral, spherical, and other crystalline phases are fused to form irregular shapes. In figure 4(c), there is still a cavity between the crystalline phase formed but in figure 4(b) it appears more tightly and crystallized.

### *3.4. FTIR analysis of $LaCrO_3$*

FTIR analysis was carried out to determine the interactions that occur between the molecular bonds of $LaCrO_3$ and molecular bonds of cellulose through vibrations produced between interactions that occur after the photocatalytic process as shown in figure 5 below.

Figures 5(a)–(c) showed spectra of a fresh $LaCrO_3$ prepared at 600, 700 and 800 °C, respectively. Typical $LaCrO_3$ peaks in the finger print area for Cr–O and O–Cr–O stretching vibrations occur at wave number of 842.4, 834.9 and 864.7 $cm^{-1}$ for $LaCrO_3$ prepared at 600, 700, and 800 °C, respectively. While the bending vibrations of La–O–La and La–O–Cr only appear clearly in $LaCrO_3$ prepared 700 °C at wave number of 772 $cm^{-1}$. Absorption in the wave number area of 3400–3100 $cm^{-1}$ states the water vapor adsorbed on the surface of the catalyst existed. Weak bending vibrations from water appear at wave numbers from 1700–1600 $cm^{-1}$. The stretching vibration that appears at wave numbers of 1500–1400 $cm^{-1}$ is probably derived from ions formed from water absorbed with the surface of La–O–Cr and Cr–O–Cr or La–O–La. Whereas the vibrations that appear at wave numbers of 1200–900 $cm^{-1}$ are probably derived from $CO_2$ adsorbed on the surface of $LaCrO_3$.

In figures 5(d) and (e) the catalyst spectra obtained after the photocatalytic reaction for $LaCrO_3$ calcined at 600 and 800 °C showed that there is an interaction between water and cellulose with the surface of the catalyst. Cellulose itself provided a stretching vibration at 3600–3100 $cm^{-1}$ for hydrogen bonds (–OH), 2900 $cm^{-1}$ for stretching vibrations –CH, 1430 $cm^{-1}$ for symmetrical bending vibrations $–CH_2$, and 898 $cm^{-1}$ for vibrations of C–O–C stretching from bonds $\beta$-(1,4)-glycosidic linkage [39, 40]. In the FTIR spectra of the $LaCrO_3$ sample obtained after the photocatalytic reaction process, it appears that the –OH stretching absorption at 3339.7 $cm^{-1}$ show that the –OH cellulose and water groups interact with the catalyst surface. Stretching vibration of the $\beta$-(1,4)-glycosidic bond appeared at wave number 1028.7 $cm^{-1}$ which also showed that there was interaction

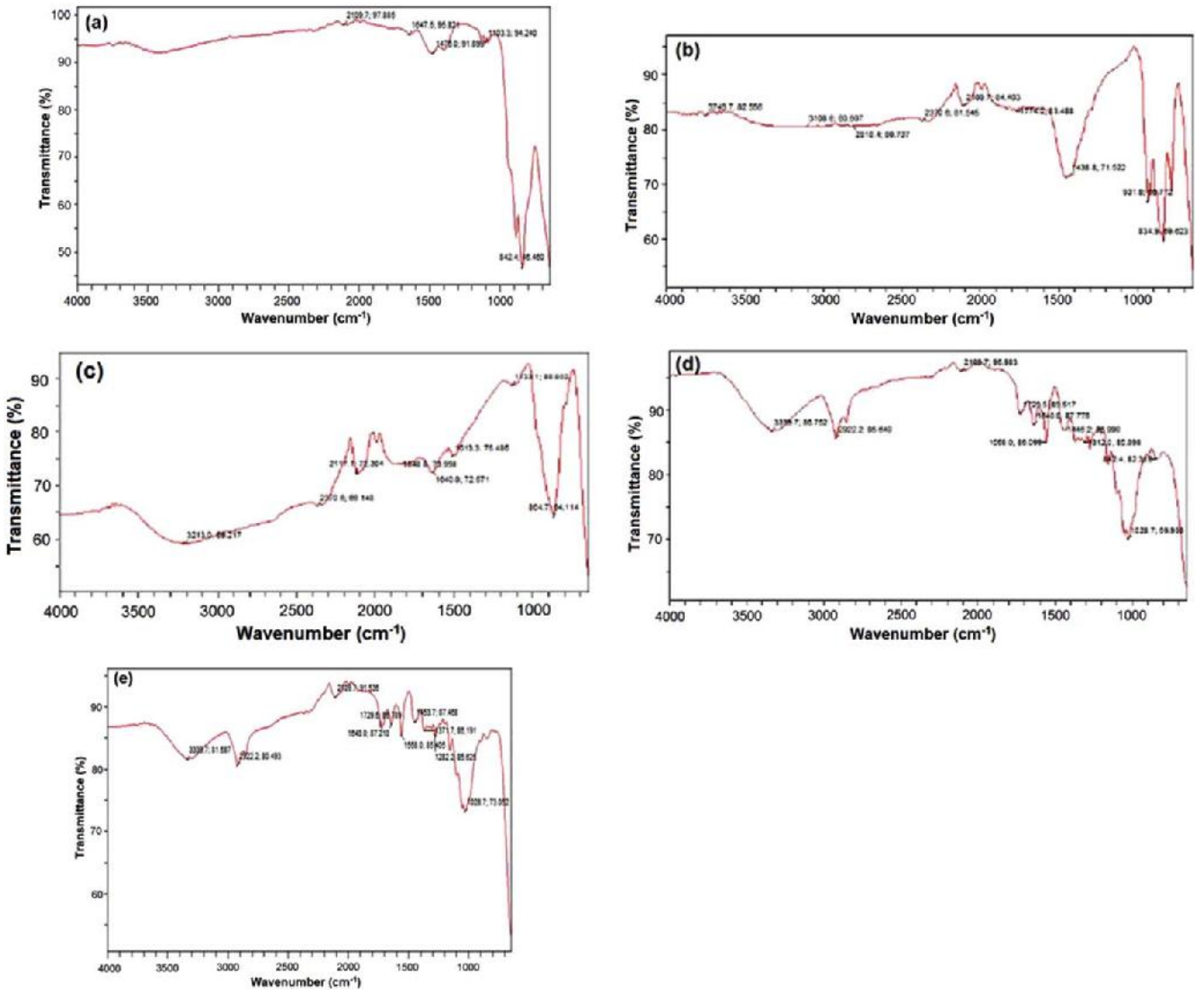


**Figure 5.** FTIR spectra of $LaCrO_3$: (a)–(c) dried samples at 600 °C, 700 °C and 800 °C, respectively; and (d), (e) samples after photocatalysis of both $LaCrO_3$ calcined at 600 and 800 °C, respectively.

with the surface of the $LaCrO_3$ catalyst. The interaction of $\beta$-(1,4)-glycosidic and $LaCrO_3$ bonds appeared relatively stronger with the catalyst being prepared at 800 °C, where transmittance for catalyst calcined at 600 °C calcined was 73% and 69.9% for $LaCrO_3$ calcined at 800 °C. Furthermore, the bending vibration peak that appears in the wave number area of 1500–995 $cm^{-1}$ states that glucose, sorbitol, mannitol and other carbohydrates are existed [41, 42]. This implies that there is a cellulose bond breakdown during the photocatalytic reaction.

### *3.5. Photocatalysis of nano cellulose*

Before carrying out chromatography analysis, samples from photocatalysis reactions were analyzed using the 3,5-dinitro salicylic acid (DNS) reagent by spectrophotometry method both qualitatively and quantitatively. Qualitatively, it was observed from the color changes shown in the process of converting cellulose to glucose in figure 6(a). Quantitatively, the concentration of reducing sugar in the solution of the conversion results was analyzed using UV–vis spectrophotometer. Measurement of concentration begins with making a curve glucose standard, where the standard glucose solution used is from 20–200 ppm and measured at a wavelength of 540 nm. Based on the calculation using linear regression equations resulting from the glucose standard curve as shown in figure 6(b), we obtained the glucose concentration of the solution for the conversion results.

Furthermore, glucose results from photocatalytic cellulose conversion are shown in figure 7 below.

In figure 7 it is clear that the catalyst calcined at 600, 700, and 800 °C is active to convert nano-cellulose under UV light irradiation. Cellulose conversion gave glucose yields over a range of 600 ppm for each exposure time applied. In detail, there is a slightly different tendency among catalysts' activity when increasing the exposure time of UV irradiation as shown in figures 7(a) and (c). However, in figure 7(b), there is an increasing yield of glucose as the exposure time increase.

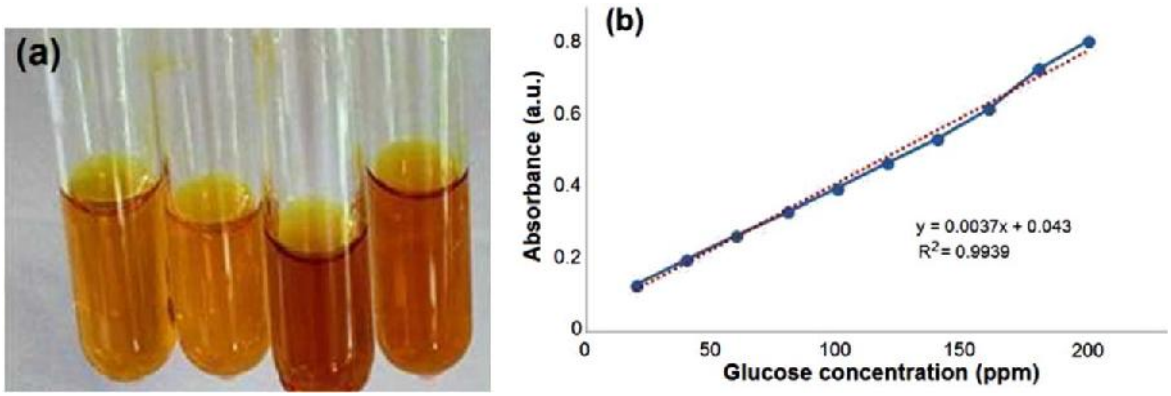


**Figure 6.** (a) The glucose resulted analyzed qualitatively by DNS, and (b) the standard glucose curve from the measurement results with the UV–vis spectrophotometer.

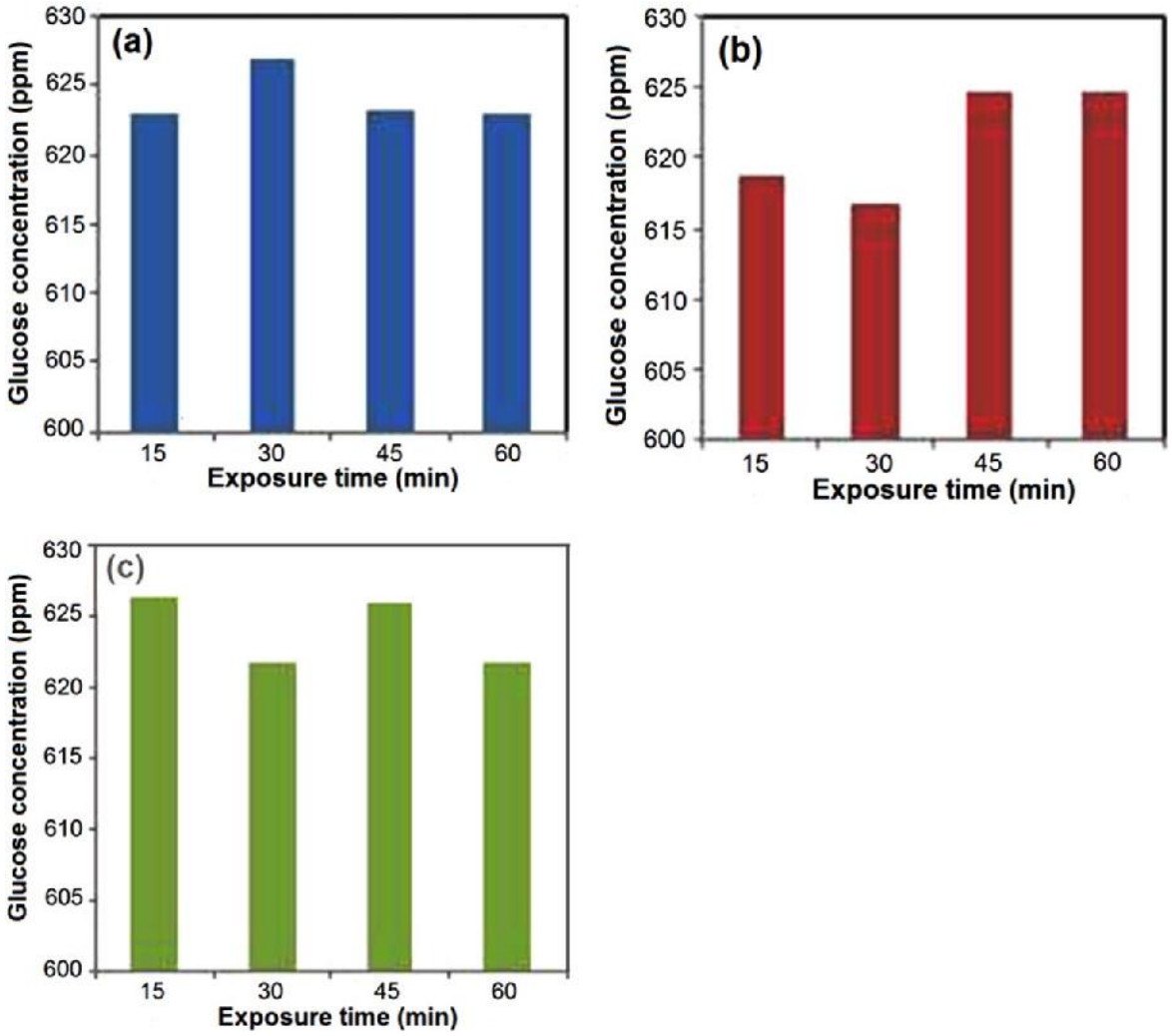


**Figure 7.** The glucose resulted by photocatalytical cellulose conversion under the UV ray irradiation of $LaCrO_3$ at (a) 600 °C, (b) 700 °C, and (c) 800 °C.

The increase in the amount of glucose as a result of the reaction when the increase in exposure time of UV irradiation happened, in general, is still relatively small compared to the amount of converted cellulose which reaches 20%–24%. So, it can be explained that the $LaCrO_3$ photocatalyst was not only acting to break the $\beta$-(1,4)-glucoside linkage of cellulose but also converting the glucose into other compounds which were not analyzed.

To determine the formation of sorbitol, mannitol, and xylitol after the photocatalytic process, the liquid sample is then analyzed using high-performance liquid chromatography (HPLC), as shown in figure 8.

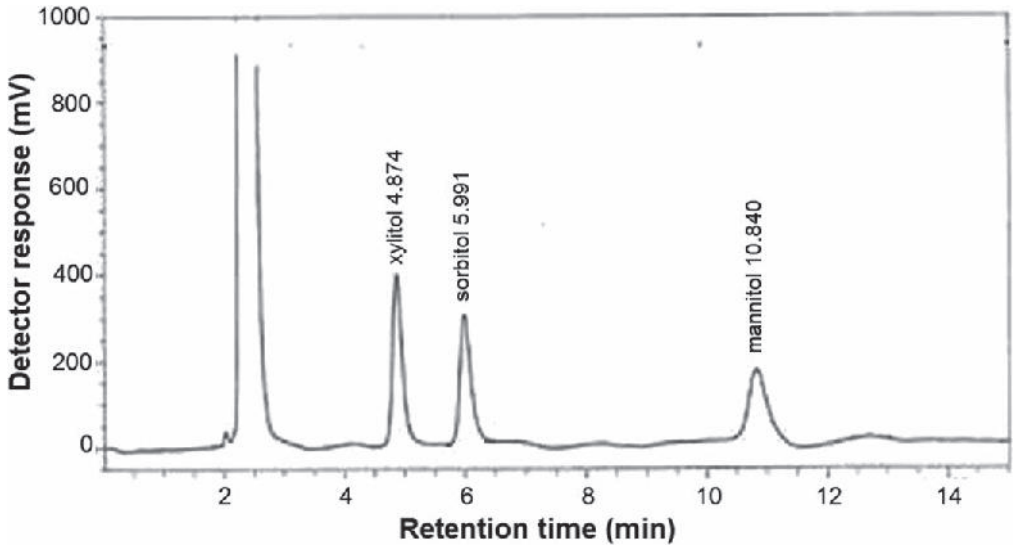


**Figure 8.** Analysis of alcohol sugar using HPLC.

**Table 1.** Distribution of alcohol sugar products as a result of the photocatalytic cellulose conversion.

| $LaCrO_3$ catalyst calcined at | Exposure time (min) | Total alcohol sugar (ppm) | Xilitol (ppm) | Sorbitol (ppm) | Mannitol (ppm) |
|---|---|---|---|---|---|
| 600 °C | 15 | 113 | 45 | 68 | — |
| | 30 | 127 | — | 87 | 40 |
| | 45 | 130 | — | 54 | 76 |
| | 60 | 172 | — | 106 | 66 |
| 700 °C | 15 | 271 | 75 | 90 | 106 |
| | 30 | 375 | 130 | 160 | 85 |
| | 45 | 620 | 260 | 210 | 150 |
| | 60 | 490 | 190 | 180 | 120 |
| 800 °C | 15 | 200 | 55 | 96 | 49 |
| | 30 | 272 | 69 | 115 | 88 |
| | 45 | 396 | 187 | 147 | 62 |
| | 60 | 262 | 101 | 84 | 77 |

By transforming the surface area of the peak using calibration curves of related alcohol sugar to the concentration, the distribution of sugar alcohol concentration as a result of cellulose conversion can be seen in table 1.

In table 1, it is clear that the length of the irradiation time will increase the production of alcohol sugar even though the $LaCrO_3$ photocatalyst calcined at 700 and 800 °C show a decrease in the alcohol sugar yield, especially at 60 min of irradiation time. This is possible because those catalysts have more capability in decomposing and binding the products.

## 4. Conclusions

Crystalline phase formation of $LaCrO_3$ perovskite was affected by the calcination temperature applied. The samples as seen by TEM is to characterize the existence of particles with varied sizes and shapes. The smallest size is less than 50 nm. In addition, SEM analysis proved that a homogeneous and hollow network were formed. The band gap energy obtained is also affected by the temperature of calcination. Its value was 2.62, 2.89, and 2.98 eV, respectively. The catalyst of $LaCrO_3$ calcined at 700 °C is active to convert cellulose with more than 620 ppm of glucose, 260 ppm of xylitol, 150 ppm of mannitol, and 210 ppm of sorbitol with the exposure time of 45 min.

## Acknowledgments

The authors wish grateful to the Research Institution of the Directorate General of Higher Education Republic of Indonesia (KEMENRISTEKDIKTI) and the Research Institution of University of Lampung (LPPM) for research funding provided through the Competitive Research Grant, with research contract No. 393/UN26.21/PN/2018. We also thanks to Prof. Taifo Mahmud, Department of Pharmacy, Oregon State University, for his advices on preparing this article.

## References


[1] Pierpaolli M, Favoni O, Fava G and Ruello M L 2018 *Method. Protoc.* **1** 1

[2] Fatima S, Ali S I, Iqbal M Z and Rizwan S 2017 *RSC Adv.* **7** 35928

[3] Rawal S B, Bera S, Lee D, Jang D-J and Lee W I 2013 *Catal. Sci. Technol.* **3** 1822

[4] Yan H, Wang X, Yao M and Yao X 2013 *Prog. Nat. Scie: Mater. Intern.* **23** 402

[5] Xiao Z, Zhou Y, Hideo H, Kamiya T and Padture N P 2018 *Chem. Eur.* J **24** 2305

[6] Sepone N and Emiline A V 2012 *J. Phys. Chem. Lett.* **3** 673

[7] Foo G S, Garzon F P, Fung V, Jiang D, Overbury S H and Wu Z 2017 *ACS Catal.* **7** 4423

[8] Situmeang R, Supriyanto R, Septanto M, Simanjuntak W, Sembiring S and Roger A C 2013 $Ni_xCo_yFe_{1-x-y}O_4$ nanocatalyst: Preparation, Characterization, and Acitvity in $CO_2/H_2$ Conversion Proc *The 2nd Int. Conf. Indones. Chem. Soc. (October 22–23th(Yogyakarta: Universitas Islam Indonesia) pp 103–10*

[9] Chawla S K, Milka G, Patel F and Patel S 2013 *Proc. Eng.* **51** 461

[10] Thuy N T, Minh D L, Giang H T and Toan N N 2014 *Adv. Mater. Scie. Eng.* **2014** 685715

[11] Moos R, Bektas M, Hanft D, Schönauer-Kamin D, Stöcker T and Hagen G 2014 *J. Sens. Sens. Syst.* **3** 223

[12] Josephine B A, Jeseentharani V, Teresita V M, George M and Antony S A 2013 *Sens. Trans.* **156** 304

[13] Liu B, Soe C M M, Stoumpos C C, Nie W, Tsai H, Lim K, Mohite A D, Kanatzidis M G, Marks T J and Singer K D 2017 *RRL Solar* **1** 1700062

[14] Chen C W, Hsiao S Y, Chen C Y, Kang H W, Huang Z Y and Lin H W 2015 *J. Mater. Chem.* A **3** 9152

[15] Pazoki M, Röckert A, Wolf M J, Imani R, Edvinsson T and Kullgren J 2017 *J. Mater. Chem.* A **5** 23131

[16] Parrey K A, Khandy S A, Laref I I A, Gupta D C, Niazi A, Aziz A, Ansari S G, Khenata R and Rubab S 2018 *J. Electro. Mater.* **47** 3615

[17] Tao S, Canales-Vázquez J and Irvine J T S 2004 *Chem. Mater.* **16** 2309

[18] Waidha A I, Lepple M, Wissel K, Benes A, Wollstadt S, Slater P R, Fortes A D and Clemens O 2018 *Dalton Trans.* **47** 11136

[19] Shinoda K, Nakajima T and Tsuchiya T 2014 *J. Ceram. Soc. Japan* **122** 415

[20] Lin J *et al* 2018 *Nat. Mater.* **17** 261

[21] Loper P, Stuckelberger M, Niesen B, Werner J, Filipic M, Moon S-J, Yum J-H, Topic M, De Wolf S and Ballif C 2015 *J. Phys. Lett.* **6** 66

[22] Xie Z, Sun S, Yan Y, Zhang L, Hou R, Tian F and Qin G G 2017 *J. Phys. Cond. Matt.* **24** 245702

[23] Guerrero A and Bisquert J 2017 *Curr. Op. Electrochem.* **2** 144

[24] Nagane S, Ghosh D, Hoye R L Z, Zhao B, Ahmad S, Walker A B, Islam M S, Ogale S and Sadhanala A 2018 *J. Phys. Chem.* C **122** 5940

[25] Kong J, Yang T, Rui Z and Ji H 2018 *Catal.Today* (In Press) (https://doi.org/10.1016/j.cattod.2018.06.045)

[26] Miao J, Sunarso J, Su C, Zhou W, Wang S and Shao Z 2017 *Sci. Rep* **7** 44215

[27] Zhang G, Ni C, Huang X, Welgamage A, Lawton L A, Robertson P K J and Irvine J T S 2016 *Chem. Commun.* **52** 1673

[28] Kasahara A, Nukumizu K, Hitoki G, Takata T, Kondo J N, Hara M, Kobayashi H and Domen K 2002 *J. Phys. Chem.* A **106** 6750

[29] Deng A, Chen J, Li H, Ren J, Sun R and Zhao L 2014 *BioRes.* **9** (2) 2717

[30] Akgul M and Kirci H 2009 *J. Environ. Bio.* **30** 735

[31] Anonymous 2014 *Tree Crop Estate Statistics of Indonesia 2014-2016* (Indonesia: Directorate General of Estate Crops Publisher, Jakarta) 12550

[32] Suryadi S, Sutriyo S, Ristina S H, Rosikhoh R and Herman H 2017 *J. Young Pharm.* **9** (1 (Suppl)) S19

[33] Istirokhatun T, Rokhati N, Rachmawaty R, Meriyani M, Priyanto S and Susanto H 2015 *Proc. Environ. Sci.* **23** 274

[34] Trisunaryanti W, Triyono T, Armunanto R, Hastuti L P, Ristiana D D and Ginting R V 2018 *Indones. J. Chem.* **18** 166

[35] Triwahyuni E, Haryanti S, Dahnum D, Nurdin M and Abimanyu H 2015 *Proc. Chem.* **16** 141

[36] Krisnandi Y K, Rasanji D G W K D, Luthfiyah S Z, Zahara Z and Sihombing R 2017 *IOP Conf. Ser.: Mater. Sci. Eng.* **188** 012059

[37] Situmeang R, Supryanto R, Kahar L N A, Simanjuntak W and Sembiring S 2017 *Orient. J. Chem.* **33** 1705

[38] Situmeang R, Sembiring S, Simanjuntak W, Sembiring Z and Yuwono S D 2019 *J.Chem. Techno. Metal.* (In Press)

[39] Zain N F M, Yusop S M and Ahmad I 2014 *J. Nutr. Food Sci.* **5** (1) 334

[40] Ciolacu D, Ciolacu F and Popa V I 2011 *Cell. Chem. Tech.* **45** 13

[41] Ibrahim M, Alaam M, El-Haes H, Jalbout A F and de Leon A 2006 *Ecl. Quím., São Paulo* **31** 15

[42] Liu Y, Chen L, Wang T, Xu Y, Zhang Q, Ma L, Liao Y and Shi N 2014 *RSC Adv.* **4** 52402